Eur. Phys. J. D **32**, 339–345 (2005)
DOI: 10.1140/epjd/e2004-00188-9

THE EUROPEAN PHYSICAL JOURNAL D

Obtaining colder ensembles of free clusters by using evaporation and recoil

K. Hansen[1], K. Wong[2], and V.V. Kresin[3,a]

[1] Chalmers University of Technology and Gothenburg University, School of Physics and Engineering Physics, 41296 Gothenburg, Sweden
[2] Department of Chemistry, University of California, Riverside, CA 92521, USA
[3] Department of Physics and Astronomy, University of Southern California, Los Angeles, CA 90089-0484, USA

Received 26 August 2004 / Received in final form 28 October 2004
Published online 21 December 2004 –

Abstract. We describe a theoretical model which treats the effects of evaporation-induced recoil on the mass and temperature distributions of a collimated beam of small neutral clusters emitted by a hot-nozzle source. The model incorporates two important consequences of in-flight cluster fragmentation processes. One is the well-known statistical evaporation of atoms and dimers accompanied by cluster size redistribution and cooling, and the other is the accompanying mechanical recoil of the fragments. We predict that the filtering effect introduced by cluster recoil can be used to an advantage by separating out the off-axis cluster population. This fraction will have a significantly narrower and colder distribution of internal temperatures than the on-axis ensemble.

PACS. 36.40.Qv Stability and fragmentation of clusters – 82.20.Db Transition state theory and statistical theories of rate constants

1 Introduction

Observations on free atomic clusters are sensitive to thermal effects. In many situations it is desirable to work with an ensemble of clusters which have as low and well-defined energy as possible. But for beams of free clusters that are generated in hot expansion sources, it is difficult to lower and control their temperature. Such is the situation, for example, with alkali clusters. For these, techniques such as the use of thermalization flow tubes [1–3], low-temperature laser vaporization [4], and the entrapment of clusters inside cold helium nanodroplets [5,6] have proven successful, but they have limitations. For example, thermalization tubes have been used with beams of alkali cluster ions and neutral particles containing $\gtrsim$50 atoms, but not with smaller clusters, whose production requires supersonic rather than condensation sources. Condensation by ^4He_n droplet pickup ensures cooling to 0.37 K, but aggregation and fragmentation-free detection of alkali species remains so far an extremely challenging problem [7].

We propose and theoretically analyze another possible method of separating an ensemble of clusters possessing both a reduced temperature and a reduced temperature distribution width. The method relies on the phenomena of evaporation and recoil. Specifically, it takes advantage of the fact that when a hot cluster flying in a beam evaporates an atom or a dimer, the resulting "daughter" cluster will have (1) a reduced internal energy and (2) a modified direction of motion due to mechanical recoil. As a result, as will be demonstrated below for the case of a jet of hot clusters produced in a supersonic expansion, if the detector blocks off the central part of the beam and focuses on the population on the periphery, the latter will be made up of evaporation products with a much lower internal temperature and a much narrower temperature distribution than the on-line population.

In Section 2, we review the statistical formalism describing evaporation from finite systems, define the beam geometry, and describe the model calculation. Section 3 presents the results and a discussion.

2 Cluster beam as a collimated evaporative ensemble

A schematic view of the basic experimental geometry addressed here is shown in Figure 1. To be specific, we discuss the case of a sodium cluster beam [8], but the general approach is applicable to a variety of systems.

A neutral cluster beam is generated in a hot source with a supersonic expansion nozzle. It passes through a skimmer and then, following a long free-flight path, enters the detector through a collimating aperture. Here the

[a] e-mail: kresin@usc.edu

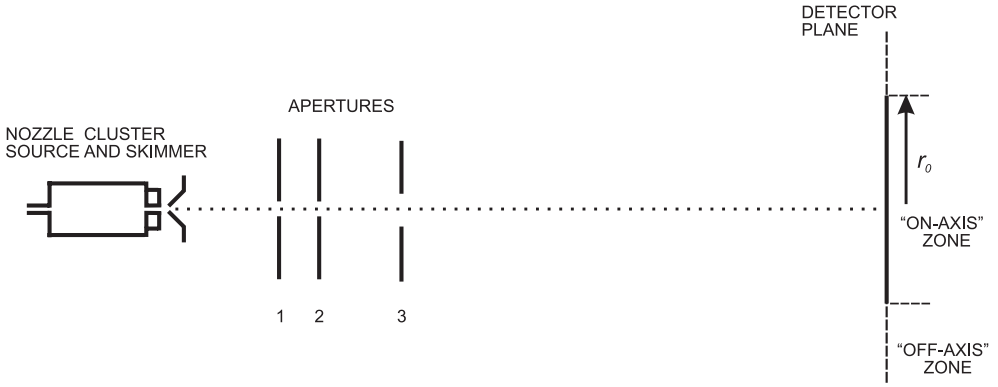

Fig. 1. Outline of the modelled beam geometry. The supersonic beam exits from a hot nozzle, passes a 0.2-mm skimmer and continues through three collimating apertures. Their distances to the nozzle and diameters are $L_1 = 0.2$ m, $L_2 = 0.3$ m, $L_3 = 0.5$ m and $D_1 = 0.8$ mm, $D_2 = 1.2$ mm, $D_3 = 2.0$ mm. The detector plane is $L_d = 2.0$ m from the nozzle. As described in the text, a radius $r_0 = 7$ mm separates the "on-axis" and "off-axis" zones.

clusters are photoionized, mass selected, and detected by an ion counter.

Our interest is in sampling the internal energies of clusters which evaporate in-flight during a well defined time interval, as the basis of a procedure to select clusters with a relatively narrow excitation energy distribution. This is accomplished by exploiting the recoil of the evaporating clusters, which positions these particles off-axis in the beam. This evaporative recoil effect has previously been put to quantitative use in studies of kinetic energy release and cluster thermometry, see, e.g., references [9–13] and references therein. To accomplish the selection we introduce three additional collimating apertures in the beamline, as shown in Figure 1, to reject the clusters which evaporate outside the desired window.

The effect of the apertures can be understood as follows. The first aperture collimates the beam. Nevertheless, since a large fraction of the cluster population undergoes evaporation before reaching this aperture (the evaporation rate strongly decreases with time), there would be some clusters able to pass through it while still possessing some transverse recoil velocity. They would make a significant contribution to the off-axis signal at the detector, but this effect is strongly reduced by the last aperture. Once these two apertures are installed, the dominant remaining uncontrolled component of the off-axis distribution would come from those clusters which pass through the first aperture under an angle and evaporate again, recoil through the last aperture and land off-axis in the detector plane. This fairly small amount is efficiently removed by adding the middle aperture.

In the simulation described below, the evaporation events are tracked as an ensemble of clusters that moves from the source to the detector plane. The coordinates of all clusters reaching the detector plane were recorded, as were the position of their last evaporation. This information allowed us to define the optimal "off-axis" detection region. Even though the greatest beam intensity is found, of course, on-axis, this signal represents a broad mixture of components from clusters with all possible evaporation histories [14]. However, off-axis one finds only those clusters which evaporate during the last stage of their flight path (almost exclusively after Aperture 2).

For the conditions analyzed here (as defined in the caption to Fig. 1), it turned out that a convenient boundary between the "on-axis" and "off-axis" regions corresponds to a radial displacement of $r_0 = 7$ mm. That is to say, we will compare the cluster populations hitting the detector plane at distances less than and greater than r_0 away from the apparatus axis. The chosen value, while relatively large, is neither impractical nor rigid. As will be shown in the next section, the assumed collimation leaves a detectable amount of flux.

Thus we wish to follow the internal energies and trajectories of the clusters as they travel from the source towards the detector. This is done by a Monte Carlo simulation, starting with an ensemble of clusters leaving the nozzle. In flight, each of them has a certain probability of evaporating an atom or a dimer. As a result of the evaporation, two things happen: (1) the cluster acquires a certain recoil velocity, and (2) its internal temperature drops, reducing the probability of further fragmentation events.

A quantitative application of this model requires several components: an expression for the fragmentation probability as a function of the cluster's internal energy E and dissociation energy D, a knowledge of the kinetic energy released when atoms evaporate from the cluster, a knowledge of the cluster dissociation energies, and an assumption about the initial thermal and spatial distributions of the beam. The first two ingredients are provided by the statistical Weisskopf formalism for nuclear evaporation [15,16] adapted to clusters [17–20]:

$$k(E,\epsilon)d\epsilon = \frac{g\mu}{\pi^2\hbar^3}\sigma(\epsilon)\ \epsilon\ \frac{\rho_{daughter}(E-D-\epsilon)}{\rho_{parent}(E)}\ d\epsilon, \quad (1)$$

where g is the spin degeneracy of the evaporating atom ($g = 2$ for sodium), ϵ its kinetic energy, μ the reduced mass of the atom and the cluster, and ρ the energy level densities of the daughter and parent cluster, as indicated. The cross-section, $\sigma(\epsilon)$, is that for the reverse process, i.e., for the capture of an atom or a dimer by a cluster.

This formula was first applied to clusters by Engelking [21] who analyzed the decay of CO_2 clusters assuming a geometric capture cross section and an energy level density $\rho \propto E^{s-1}$, where s is the number of vibrational modes. This form represents the level density for a collection of harmonic oscillators in the high temperature limit, i.e., when the energy per degree of freedom is significantly higher than the vibrational energy quantum. It is known in molecular physics as the Kassel model [22]. That is, it is assumed that the thermal excitation energy is shared between $s = 3n-6$ harmonic vibrational modes. A special case is that of the Einstein model where all frequencies are identical, $\nu_i = \nu$ [23].

Neither the Einstein nor the Kassel model are very accurate for hot, especially molten, clusters. However, as shown in [18,20], for alkali metals the inaccuracies appear to compensate each other and yield results close to those given by more quantitatively elaborate models. A more important reason for adopting this approximation here is the fact that the dissociation energies which will be employed below have been extracted from experimental data by using precisely this level density parametrization [24]. Thus the errors will cancel out to a degree, and using other parametrizations [18,25] and more realistic caloric curves [26] here would be neither self-consistent nor more precise.

For the same reason we use the same expression for the dimer evaporation rate constant as for the monomer. It is well-known that the frequency factors for the two cases are not the same because of different phase space factors [27], but if this difference were included without modifying the dimer binding energies [24], it would lead to too high a dimer evaporation rate and to a serious overestimate of recoil effects for certain cluster sizes.

Additionally, for thermal evaporation of neutral fragments from neutral clusters the capture cross section can be taken to be approximately independent [10] of ϵ and equal to the geometrical cross section (i.e., a unity sticking coefficient).

With the above approximations, the expression for the evaporation rate constant of the n-atom cluster becomes

$$k_n = 8\pi\sigma\mu\nu^3(3n-7)\frac{(E-D_n)^{3n-8}}{(E)^{3n-7}}. \qquad (2)$$

As mentioned, the cluster dissociation energies D_n ($\sim$0.6$-$1.2 eV) are taken from the measurements of Bréchignac et al. [24] on Na_n^+ ions. Since the stabilities of simple metal clusters are governed by the number of valence electrons, we take $D(Na_n) \approx D(Na_{n+1}^+)$. As there have been no measurements of dissociation energies for neutral alkali clusters in this size range, an alternative would be to invoke a Born-Haber cycle to calculate these numbers from the cluster ionization potentials (IP) [4,28,29]. The results are close (generally, within the experimental IP scatter) to the isoelectronic ion values [29], so using the latter for $D(Na_n)$ is a reasonable approximation. Finally, the frequency ν in equation (2) is taken to be the Debye frequency of the solid metal, as in [24].

In addition to the evaporation rate, a calculation focusing on recoil effects requires information on the distribution of kinetic energies of the atom. From equation (1), irrespective of the precise functional form of the level density, this distribution can to a good approximation be expressed as [18]

$$I(\epsilon)d\epsilon = A\epsilon e^{-\epsilon/k_BT}d\epsilon, \qquad (3)$$

(assuming an energy-independent σ). Here T, the temperature of the daughter cluster, is used as a measure of its internal energy contents [15,16]:

$$\frac{1}{k_BT} \equiv \frac{\partial(\ln\rho)}{\partial E}. \qquad (4)$$

For a system of harmonic oscillators, T is related to the thermal excitation energy via [30] $E = (3n-6)k_BT$. To reiterate, this approximation is made in order to be consistent with the choice adopted in [24].

The simulation launched clusters from the $z = 0$ (source) plane with initial velocity and spatial distributions described below. While in flight, the clusters were allowed to decay by monomer and dimer evaporation, with the branching between the two channels decided randomly with probabilities given by the relative magnitudes of the two rate constants. The distribution of evaporation kinetic energies was generated according to equation (3) with standard procedures [32]. The recoil velocities were generated by multiplying the evaporation speed by an isotropically distributed unit vector, and scaling to obtain the daughter cluster velocity. At the end of the flight path, clusters reaching the detector plane were binned according to their mass, the distance from the beam axis, and the internal energy. Typically, 10^8 clusters were launched in each simulation with $\sim$10% of the total reaching the detector plane and between 1$-$15% (depending on the cluster size) of the latter amount landing in the "off-axis" zone.

The starting distributions of cluster mass, temperature, and flow ideally would come from a model of the cluster formation process, but the present state of the theory is far from being able to provide such details [33–36]. The most effective approach to date remains the semi-empirical description given by Hagena [37]; this picture describes the basic parameters under which nucleation can take place, but does not give values for the abundance spectra to be expected. We therefore adopt some simple schematic initial conditions which are adequate for a characterization of the proposed picture.

For the original cluster population, we assume a simple rectangular distribution of cluster abundances from $n = 5$ to $n = 35$. For the initial temperature distribution, we similarly take a rectangular distribution centered around $T_0 = 900$ K, which is slightly above the typical temperature of a supersonic alkali cluster source reservoir due to the additional heating induced by passage through the hot nozzle and by the heat of cluster condensation. A precise value is very difficult to establish with confidence but the simulation is not very sensitive to this parameter.

The width of the distribution is calculated as [38–40]

$$k_B \Delta T_n \approx \frac{D(\mathrm{Na}_n)}{3n-6}. \quad (5)$$

This gives us, for example, a width of ±100 K for Na_{20}.

Finally, we need to define the geometrical trajectories followed by the newly condensed clusters as they leave the formation zone in (or very close to) the nozzle [34,35]. In principle, this is an extraordinarily complicated fluid-dynamical problem involving motion along expansion flow lines, collision processes, longitudinal and transverse velocity distributions, and other entanglements.

We define an elementary geometry which aims to reflect the fact that collisions with the carrier gas may effectively diminish cluster recoil following fragmentation. Thus clusters that evaporate heavily in the proximity of the nozzle are prevented from leaving the beam and are kept along the pathway of the expansion streamlines. In order to simulate this effect, we introduce a "constrained expansion length" l_c: the clusters evaporate freely while within l_c of the nozzle, but are constrained to move in the forward direction. The value chosen here, $l_c \approx 0.1$ mm, is about 30% larger than the diameter of the nozzle and fits with the fact that for an axially symmetric expansion the number of constraining collisions decreases very rapidly with the distance to the nozzle [35].

After this first stage, the resulting cluster mass and temperature distributions are used as a starting point for the second stage. The second stage of the cluster path is approximated by distributing the cluster population uniformly within the skimmer opening and assigning to it a transverse velocity spread equal to the width of the experimentally measured longitudinal velocity distribution [41] ($\langle v_\parallel \rangle = 1100$ m/s, $v_\perp \approx \Delta v_\parallel = 150$ m/s). This picture is close to the wide virtual source concept as described in reference [42]. During this second stage, which terminates at the detector plane, the clusters move freely between evaporations within the constraints imposed by the apertures [43].

It should be clear that the main physical mechanism addressed in the paper, i.e., the significant cooling and narrowing of the cluster internal energy distribution, is quite general and does not depend on the specific assumptions of the simulation.

3 Results

Figure 2 compares the modelled abundance spectra of the "on-axis" and "off-axis" ensembles. While shell edge effects are visible in both, the position of the "center of mass" and other details differ significantly. An observation of such differences could serve as an experimental test of the predicted behavior. Note that even though in the present geometry the off-axis intensity is approximately an order of magnitude weaker than the on-axis one, it should remain readily detectable in a cluster beam apparatus.

The inset in Figure 2 shows a typical experimentally measured mass spectrum in a supersonic alkali cluster beam apparatus [45]. The simulation of on-axis intensities correctly describes the rearrangement of the initially smooth size distribution into a shell pattern. A more precise match to the experimental data calls for an improved knowledge of the starting distribution of nucleated clusters and of neutral cluster dissociation energies [46].

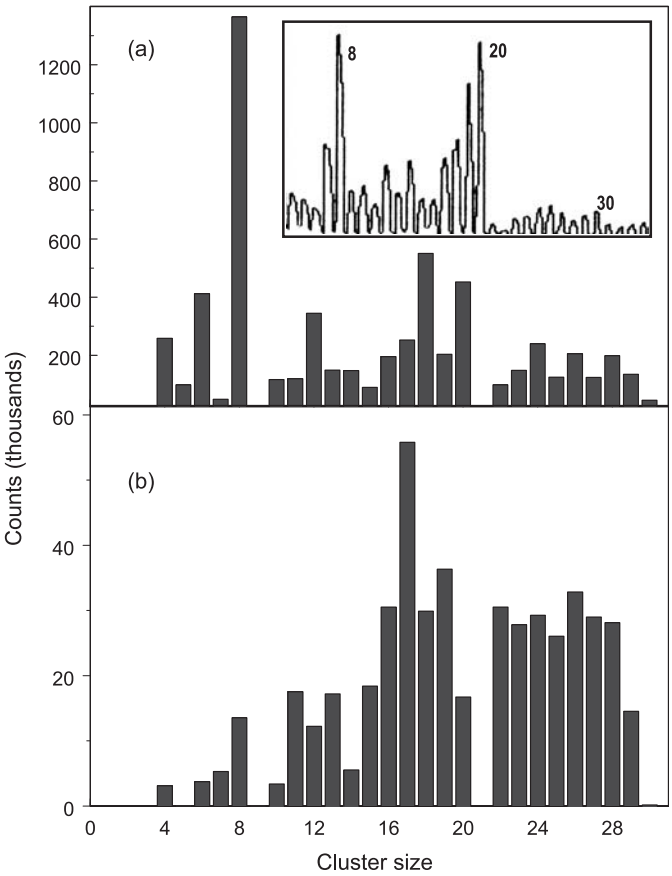

Fig. 2. A comparison of the "on-axis" (a) and "off-axis" (b) cluster abundance spectra modelled as described in the text. The variations in abundances are created by in-flight evaporation, as the initial distribution emitted by the source was assumed to be flat from Na_5 through Na_{35}. Insert: an experimental sodium cluster mass spectrum [45] (optimized for enhanced production in the $Na_8 - Na_{20}$ size range).

Figure 3 compares the widths of the internal energy distribution calculated for some selected cluster sizes arriving at the detector. It can be seen immediately that, as expected, the off-axis distribution is noticeably narrower than the on-axis one, and its center is shifted towards lower energies. This is summarized in Figure 4 for the entire modelled population.

The following calculation can account for the behavior of the widths. The energy distribution of the full ensemble of daughters (clusters detected on- and off-axis) will have approximately the same width as the parent ensemble: on the order of the dissociation energy, cf. equation (5). The width of the on-axis distribution will be only slightly less, and can therefore be estimated as

$$\Delta E_{on-axis} \sim D/\sqrt{12}, \quad (6)$$

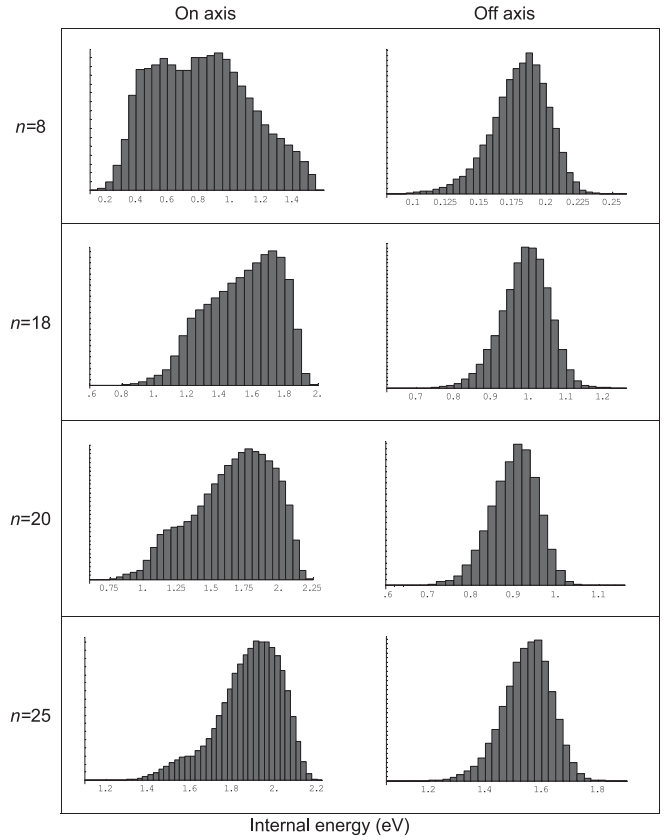

Fig. 3. Histograms of the internal energy distributions of several cluster sizes reaching the detector plane at a distance less (left column) and greater (right column) than r_0 from the beam axis. Note the different energy scales of the two columns. The narrowing and cooling of the distribution is due to the recoil effect as discussed in the text.

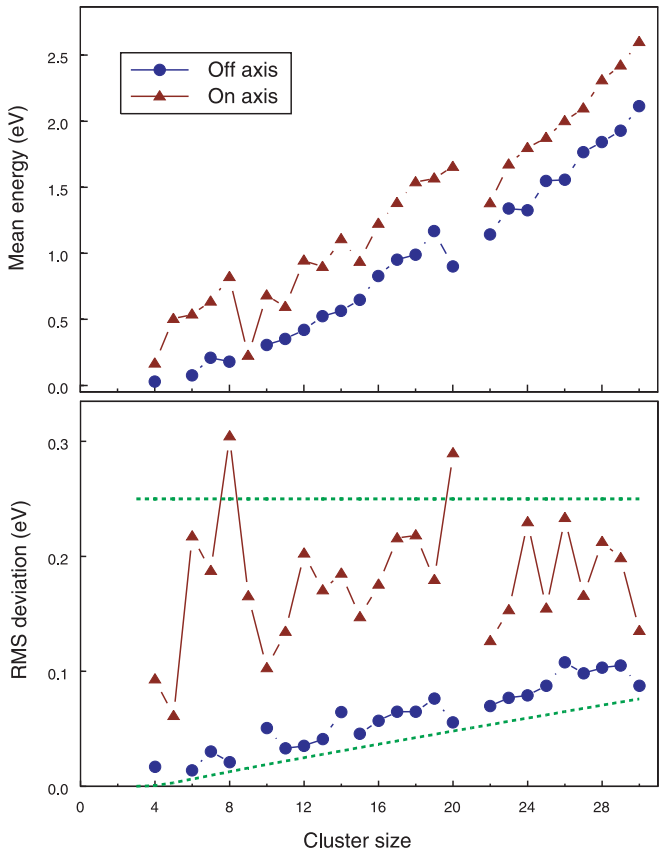

Fig. 4. Mean values (top) and standard (RMS) deviations (bottom) of the calculated internal energy distributions of sodium clusters reaching the detector plane. A significant cooling and width reduction is evident for the recoiled off-axis clusters. Dashed lines: theoretical estimates, equations (6, 9), of the expected root-mean-square energy distribution widths for the clusters detected on- and off-axis.

where D is the average dissociation energy. The square root appears as the root-mean-square (RMS) deviation of a simple rectangular distribution. With $D \sim 0.9$ eV, this estimate yields $\Delta E_{on-axis} \sim 0.25$ eV, close to the RMS widths of the simulated values. This estimate could be further improved by accounting for parent-daughter dissociation energy differences [40], i.e., shell effects (thus introducing oscillations about the mean value of $\Delta E_{on-axis}$) and by including the dimer evaporation channel.

The off-axis internal energy distributions are significantly narrower than the on-axis ones, because the former ensemble consists just of those clusters which evaporate during a narrow time window. It is narrow in the sense that it covers only a factor of four in the flight time, which is to be compared with the tremendous difference between the intrinsic scale of the evaporation rate constants (on the order of 10^{-15} s) and the time it takes the beam to reach the collimating apertures ($t_0 \sim 1$ ms). (Note, therefore, that the narrowing effect is rather general. For example, it can also be achieved with beams of cluster ions by appropriate gating.)

Because the rate constant $k(E)$ is strongly dependent on the internal energy, the population of clusters which evaporates between the collimation apertures (and thereby contributes to the off-axis signal) is narrowly localized in energy: it includes only those clusters for which

$$k(E)t_0 \approx 1. \tag{7}$$

Clusters with a higher (lower) internal energy contents evaporate too early (too late). To make this argument more quantitative and to derive an estimate for the width of the corresponding energy distribution, consider that the latter can be represented by the "survival function", $P(E) = \exp[-k(E)t_0]$. (The skewness caused by dimer decay results in minor modifications which, as for the on-axis distributions, need not be considered here.) As was just stated, this function exhibits a rapid crossover from 1 to 0 at a certain value of the internal energy. The energy distribution of the *recoiled* clusters can therefore be calculated from the width of this crossover region.

The condition (7) corresponds to the inflection point of $P(E)$. To a first approximation, then, the width of the crossover region can be taken to be $\Delta P/(dP/dE) = -1/(dP/dE)$, with the derivative evaluated at the inflection point. Approximating the rate constant (2) for

sufficiently large n as

$$k(E) \approx \omega \left(1 - \frac{D}{E}\right)^{3n-7}, \tag{8}$$

we can calculate the RMS energy spread as

$$\Delta E_{off-axis} \approx \frac{1}{\sqrt{12}} \frac{-1}{dP/dE} = D \frac{e}{\sqrt{12}(3n-7)} \frac{x}{(x-1)^2}, \tag{9}$$

where $x = (\omega t_0)^{1/(3n-7)}$. Inserting $\omega \approx 10^{15}$ s^{-1}, $t_0 \approx 10^{-3}$ s, and $D \approx 0.9$ eV, we obtain the lines shown in Figure 4. The RMS width is found to grow approximately linear with n, after an onset below $n = 3$, in good agreement with the simulation model.

4 Conclusions

We have described a model analyzing the energy distributions and abundance spectra of clusters generated by hot evaporative sources. It accounts for two concomitant thermal effects: (a) evolution of cluster sizes and temperatures through evaporation cascades ("evaporative ensemble" theory), as well as (b) evaporation-induced cluster recoil. The second effect can be put to use in order to control the shape of the internal energy distribution of a cluster beam.

A simple geometrical model for the production and flow of the initial cluster distribution achieves a reasonable reproduction of the experimental mass spectra. Furthermore, it is shown that by using realistic beam collimation parameters it is possible to reduce the width of the temperature distribution of arriving clusters by as much as a factor of 2−10, and to shift it towards significantly lower temperatures. This effect is due to a bias introduced by the recoil ejection of fragment clusters. It is predicted, therefore, that the details of mass and temperature distributions of cluster beams can be modified by varying the beam collimation parameters.

We would like to thank P. Brockhaus for motivating and originating these calculations. The work of K.H. was supported by the Swedish Research Council (VR). The work of V.K. was supported by the U.S. National Science Foundation (Grant No. PHY-0354834).

References

1. H. Haberland, in *Metal Clusters*, edited by W. Ekardt (Wiley, New York, 1999)
2. T. Bergen, X. Biquard, A. Brenac, F. Chandezon, B.A. Huber, D. Jalabert, H. Lebius, M. Maurel, E. Monnand, J. Opitz, A. Pesnelle, B. Pras, C. Ristori, J.C. Rocco, Rev. Sci. Instrum. **70**, 3244 (1999)
3. J. Borggreen, K. Hansen, F. Chandezon, T. Døssing, M. Elhajal, O. Echt, Phys. Rev. A **62**, 013202 (2000)
4. M.L. Homer, J.L. Persson, E.C. Honea, R.L. Whetten, Z. Phys. D **22**, 441 (1991)
5. S. Vongehr, A.A. Scheidemann, C. Wittig, V.V. Kresin, Chem. Phys. Lett. **353**, 89 (2002)
6. C.P. Schulz, P. Claas, D. Schumacher, F. Stienkemeier, Phys. Rev. Lett. **92**, 013401 (2004)
7. S. Vongehr, V.V. Kresin, J. Chem. Phys. **119**, 11124 (2003)
8. W. de Heer, W. Knight, M.Y. Chou, M.L. Cohen, in *Solid State Physics*, edited by H. Ehrenreich, D. Turnbull (Academic, New York, 1987), Vol. 40
9. K. Hansen, J. Falk, Z. Phys. D **34**, 251 (1995)
10. P. Brockhaus, K. Wong, K. Hansen, V. Kasperovich, G. Tikhonov, V.V. Kresin, Phys. Rev. A. **59**, 495 (1999)
11. C. Lifshitz, Int. J. Mass Spec. **198**, 1 (2000)
12. C. Bréchignac, Ph. Cahuzac, B. Concina, J. Leygnier, B. Villard, P. Parneix, Ph. Bréchignac, Chem. Phys. Lett. **335**, 34 (2001)
13. K. Głuch, S. Matt-Leubner, O. Echt, R. Deng, J.U. Andersen, P. Scheier, T.D. Märk, Chem. Phys. Lett. **385**, 449 (2004)
14. This signal includes unevaporated clusters from the original population, as well as all those daughters which recoil in the forward direction. And although the fraction of such daughters quickly falls off with the distance from the detector plane (i.e., for evaporation at early flight times), the evaporation rate at the early time is significantly higher. To a significant extent, the two effects cancel each other and turn the energy contents of the on-axis beam into a rather broad mixture
15. J.U. Blatt, V.F. Weisskopf, *Theoretical Nuclear Physics* (Wiley, New York, 1952)
16. T. Ericson, Adv. Phys. **9**, 425 (1960)
17. G.F. Bertsch, N. Oberhofer, S. Stringari, Z. Phys. D **20**, 123 (1991)
18. S. Frauendorf, Z. Phys. D **35**, 191 (1995)
19. P.A. Hervieux, D.H.E. Gross, Z. Phys. D **33**, 295 (1995)
20. P. Fröbrich, Ann. Physik (Leipzig) **6**, 403 (1997)
21. P. Engelking, J. Chem. Phys. **87**, 936 (1987)
22. P.J. Robinson, K.A. Holbrook, *Unimolecular reactions* (Wiley, London, 1972)
23. N.W. Ascroft, N.D. Mermin, *Solid State Physics* (Holt, Rinehart and Winston, New York, 1976)
24. C. Bréchignac, Ph. Cahuzac, J. Leygnier, J. Weiner, J. Chem. Phys. **90**, 1492 (1989)
25. C. Walther, G. Dietrich, W. Dostal, K. Hansen, S. Krückeberg, K. Lützenkirchen, L. Schweikhard, Phys. Rev. Lett. **83**, 3816 (1999)
26. M. Schmidt, J. Donges, Th. Hippler, H. Haberland, Phys. Rev. Lett. **90**, 103401 (2003)
27. K. Hansen, Philos. Mag. B **79**, 1413 (1999)
28. M.M. Kappes, M. Schär, E. Schumacher, A. Vayloyan, Z. Phys. D **5**, 359 (1987)
29. Ph. Dugourd, D. Rayane, R. Antoine, M. Broyer, Chem. Phys. **218**, 163 (1997)
30. The energy-temperature relation for a microcanonical ensemble is better represented if $(3n - 6)$ is replaced by $(3n - 7)$ [31] but this point has only a minor influence on the recoil calculation
31. J.U. Andersen, E. Bonderup, K. Hansen, J. Chem. Phys. **114**, 6518 (2001)
32. *Handbook of Mathematical Functions*, edited by M. Abramowitz, I.A. Stegun (Dover, New York, 1965)
33. M. Kappes, S. Leutwyler, in *Atomic and Molecular Beam Methods*, edited by G. Scoles (Oxford, New York, 1988)
34. G.D. Stein, Surf. Sci. **156**, 44 (1985)

35. S.B. Ryali, J.B. Fenn, Ber. Bunsenges. Phys. Chem. **88**, 245 (1984)
36. H. Pauly, *Atom, Molecule, and Cluster Beams* (Springer, Berlin, 2000)
37. O.F. Hagena, Surf. Sci. **106**, 101 (1981); O.F. Hagena, Z. Phys. D **4**, 291 (1987)
38. C.E. Klots, J. Chem. Phys. **83**, 5954 (1985); C.E. Klots, J. Phys. Chem. **92**, 5864 (1988); C.E. Klots, Z. Phys. D **21**, 335 (1991)
39. U. Näher, K. Hansen, J. Chem. Phys. **101**, 5367 (1994)
40. K. Hansen, U. Näher, Phys. Rev. A **60**, 1240 (1999)
41. G. Tikhonov, K. Wong, V. Kasperovich, V.V. Kresin, Rev. Sci. Instrum. **73**, 1204 (2002)
42. H. Beijerinck, N. Verster, Physica **111C**, 327 (1981)
43. The free-flight trajectories of cluster parents and daughters may, in principle, be deflected by collisions with background gas in the vacuum chambers and with the carrier gas atoms. As mentioned in the text, the primary contribution to the off-axis signal comes from clusters evaporating after Aperture 2, so the concern is whether scattering in this region may distort the pattern created by evaporative recoil. Such scattering will be dominantly of the elastic van der Waals type, and the relevant cross sections have been studied in reference [44]. From the data in this reference, it follows that the "extinction length" for scattering a fraction $1/e$ of the clusters into an angle of 4 mrad (the angle subtended by the radius r_0 in the detector plane as seen from Aperture 2) by a pressure P of Ar or N_2 is ≈ 5 mm/$P(10^{-3}$ mbar). This means that with chamber pressures of $\gtrsim 10^{-8}$ mbar following Aperture 2, only a fraction of one percent of the parent clusters will be scattered beyond r_0 by the background gas. Note that the carrier gas which accompanies the beam will not scatter the parents, as they travel at close speeds. This carrier gas can, in principle, scatter the deflecting daughters, but an estimate of its pressure remaining in the beam at this point [36] yields $\sim 10^{-5}$ mbar. Only a negligible fraction of the daughter clusters will be deflected after traversing the ~ 1 mm radius of this beam. Thus we see that background and carrier gas scattering will not alter the calculated off-axis populations by more than a few percent
44. V.V. Kresin, A. Scheidemann, J. Chem. Phys. **98**, 6982 (1993)
45. W.D. Knight, K. Clemenger, W.A. de Heer, W.A. Saunders, M.Y. Chou, M.L. Cohen, Phys. Rev. Lett. **52**, 2141 (1984)
46. The dissociation energies of neutral clusters are obviously somewhat different from the ionic cluster data used in our calculations. This is well illustrated by taking the example of the Na_{21} cluster. In the experimental mass spectra, this unit has an abundance of about 10% of Na_{20}, but in the simulation it does not appear at all. This is due to the dissociation energies assigned to the Na_{22} cluster. For the reaction $Na_{22} \rightarrow Na_{20} + Na_2$, the value inferred from Na_n^+ data in reference [24] is $D = 0.65$ eV, whereas monomer dissociation is not quoted at all, thus not allowing the reaction $Na_{22} \rightarrow Na_{21} + Na$. Consequently, the simulation leaves no signal in the $n = 21$ channel. It would be interesting to reevaluate the dissociation energies of neutral clusters by combining experimentally measured mass spectra (corrected for ionization efficiency effects) and the evaporation model (cf. adjustments of Li_n^+ separation energies described in Ref. [47])
47. S. Bjørnholm, J. Borggreen, H. Busch, F. Chandezon, in *Large Clusters of Atoms and Molecules*, edited by T.P. Martin (Kluwer, Dordrecht, 1996)